Hierarchical MPC of Hybrid Power Systems based on Fuzzy Discrete Abstraction

Jianhua Zhang*, Jiajun Xia**

* Dept. of Computer Science, Oslo Metropolitan University, 0166 Oslo, Norway (e-mail: jianhuaz@oslomet.no)
** School of Information Science and Engineering, East China University of Science and Technology, Shanghai 200237, China (e-mail: genius901028@163.com)

Abstract: A hierarchical control approach is proposed for hybrid systems with discrete-valued input based on fuzzy discrete abstraction and model predictive control (MPC) scheme. The system is firstly abstracted to a discrete event system (DES). Then a higher-level supervisor is designed to provide the control input alphabet for each discrete state, while a fuzzy model predictive controller is developed for the original system in the lower level. Simulation results of emergency frequency control of electric power systems are provided to show the superior frequency recovery characteristic of the proposed hierarchical control scheme in comparison with two existing control methods.

Keywords: Hierarchical control; Fuzzy discrete abstraction; Fuzzy model; Model predictive control; Hybrid system; Discrete event system.

1. INTRODUCTION

In recent years, one of the most important research topics in the area of hybrid dynamic systems is the design of hybrid system whose input is restricted to the discrete-valued (or symbolic) signals (Minami, 2016). Discrete-valued control is a control mechanism that achieves control objectives with control actions taking values in a finite alphabet (e.g., bang-bang control) (Ikeda, Nagahara and Ono, 2017). This kind of control signals commonly exists in many types of control systems, such as mechanical systems, chemical plants, and networked systems (Azuma and Sugie, 2008). In these systems, there are usually interactions between different components in different forms, such as continuous plant output and discrete control symbols, giving rise to a *hybrid* phenomenon. This is partly due to that the dynamics of various devices embedded in these systems are discrete in nature, such as D/A converters, PWM amplifiers, and ON/OFF actuators. The discrete-valued control possesses advantages in networked control (no quantization error occurs), and it also has important applications to, for example, power systems (Woon, Rehbock and Loxton, 2012), automatic train control (Howlett, 2000), and biological systems (Azuma and Sugie, 2008). Take emergency control in power systems as an example, the under frequency load shedding (UFLS) and under voltage load shedding (UVLS) schemes are typical discrete-valued control: the loads to shed are always discrete-valued, either large or small.

Model predictive control (MPC) has been in wide use in various industrial domains, e.g. power systems, power electronics, and fuel cell control (Thomas, 2012). Wang and Mendel (1992a) proved mathematically that with a sufficient number of fuzzy partitions and fuzzy rules, a fuzzy system, whose output can be expressed explicitly as a linear combination of fuzzy (Gaussian) basis functions, can approximate any real-valued continuous function defined on a compact set to arbitrary accuracy. Intuitively, we could use fuzzy model in MPC, constituting fuzzy model predictive control. For hybrid systems with solely discrete control input, a finite-set MPC algorithm was proposed to reduce the computational cost (Thomas, 2012). The predictive procedure in the algorithm is achieved by mixed-integer programming (MIP) proposed in Bemporad and Morari (1999). In practice, mixed-integer linear/quadratic programming (MILP/MIQP) is commonly used. Those optimization methods directly yield desired control. However, the excessive computational load impedes their application to large-scale systems and hybrid systems (Thomas, 2012), since the programming problem is NP-hard and the time required to solve the problem grows exponentially with the scale of the problem (for example, the size of control input alphabet).

Besides, in the viewpoint of discrete event system (DES), the control input alphabet consists of so-called "events". Supervisory control theory (SCT), proposed by Ramadge and Wonham (1987; 1989), has been widely applied to DES and hybrid systems. For large-scale complex systems, modular SCT (Wonham and Ramadge, 1988) and hierarchical SCT (Feng and Wonham, 2008) were proposed in order to reduce the computational overhead. SCT divides the events in alphabet into controlled and uncontrolled categories, and the controlled events can be enforced or disabled for each (discrete) state depending on specifications. In this way, the size of control input is reduced for a certain (discrete) state.

In this paper, we propose a hierarchical control approach for hybrid system with discrete inputs. The system is firstly abstracted to a DES. Then a supervisor is designed in the higher level to provide the (legal) control input alphabet (subset of original alphabet) for each discrete state, while in the lower level a fuzzy model predictive controller processes the sub-alphabets (with reduced computing overhead) and outputs an optimal control input to original plant.

2. HIERARCHICAL CONTROL APPROACH

In this section, a hierarchical control approach is proposed for hybrid dynamical systems. The hierarchical structure consists of two layers: high-level supervisor and low-level fuzzy predictive controller. The block diagram of the closed-loop system is shown in Fig. 1. Depending on different discrete states, the parameters of fuzzy predictive controller may vary.
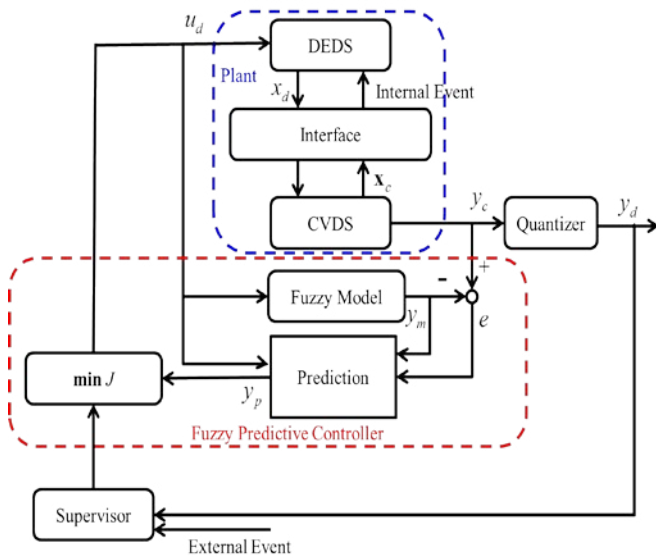

Fig. 1. General configuration of the hierarchical control system.

2.1 Fuzzy Predictive Control

A general fuzzy predictive control scheme is illustrated in the dashed red module in Fig. 2. In fuzzy model predictive control system, fuzzy model is used to represent hybrid system.

A. Fuzzy model

The fuzzy model component in Fig. 1 functions as a function approximator of the plant under control. The fuzzy model comprises a set of fuzzy rules with properly defined membership functions (MFs) and defuzzification approach.

The physical model of complex system is usually hard to obtain. However, the I/O data pairs of the complex plant are relatively easy to acquire, hence data-driven modeling methods can be applied. In this work, a widely-used fuzzy modeling approach, namely Wang-Mendel (WM) method, is used to build fuzzy model from the I/O sample data. A detailed description of WM method can be found in Wang and Mendel (1992b) and Wang (2003).

For fuzzy modeling, Gaussian MFs are adopted, whose parameters can be optimized with evolutionary algorithms. With data-driven modeling and parameter optimization procedure, a fuzzy rule base can be elicited along with appropriate defuzzifier for fuzzy reasoning.

With the fuzzy rule base and defuzzifier (Zhang, Xia and Wang, 2018), we can obtain the analytical description of the plant under control as:

$$\hat{y}_c = F(\mathbf{x}_c, x_d). \tag{1}$$

where $\hat{y}_c$ is the model output.

B. Prediction

With the fuzzy model and future control input, prediction can be made. Intuitively, an open-loop prediction is:

$$y_p(k+i) = \hat{y}_c(k+i) = F(\mathbf{x}_c(k+i), x_d(k+i)), i = 1, 2, \cdots, P \tag{2}$$

where P is the prediction horizon. However, there always exists error between the model and measured output. In order to eliminate the steady-state error between them, we modify (2) as:

$$y_p(k+i) = \hat{y}_c(k+i) + e(k), i = 1, 2, \cdots, P, \tag{3}$$

where $e(k)$ is the error term:

$$e(k) = y_c(k) - \hat{y}_c(k), \tag{4}$$

C. Optimization

With the prediction result, the optimization of performance index w.r.t. input(s) can be performed. The performance index is defined as:

$$\min J(k) = \sum_{i=1}^{P} \left(G\left(\mathbf{x}_c(k+i), x_d(k+i) \right) \right) \tag{5}$$

where $G(\cdot)$ is a function of $\mathbf{x}_c$, x_d, and implicitly y.

For tracking problem, the performance index becomes:

$$\min J(k) = \sum_{i=1}^{P} \omega_i \left(y_p(k+i) - y_r(k+i) \right)^2 \tag{6}$$

where y_r is the reference output to be tracked and ω_i the weights.

The optimal discrete-valued input sequence can be obtained by MILP/MIQP.

2.2 Supervisory Control

Supervisory control theory was proposed for DES by Ramadge and Wonham (1987; 1989). The input symbols of DES ("events") are divided into two disjoint parts: controlled events and uncontrolled ones. The occurrence of controlled events could be prevented, whereas the uncontrolled ones could not. Take power system as an example, generator fault is an uncontrolled event; load shedding is a controlled event. The supervisor can prevent (or enforce) the controlled events from happening (or to happen) according to design needs.

In this paper, we adopt the SCT methodology. The supervisor here serves as a high-level regulator: for different discrete states of the hybrid system, some controlled events can be prevented and hence removed from the input alphabet. The computational load is hence reduced even when the optimization procedure in MPC is combinatorial of all possible inputs. For multi-task control problems or complex

systems, a modular SCT approach was proposed to split the control tasks to several sub-tasks and then design "sub-supervisor" for each sub-task. As long as the behavior languages of "sub-supervisors" are non-conflicting and non-blocking, input alphabet can be further reduced by intersection of the sub-alphabets (Wonham and Ramadge, 1988).

3. APPLICATION TO EMERGENCY FREQUENCY CONTROL OF POWER SYSTEMS

3.1 Power Systems

Power systems are typical hybrid dynamical systems. The currents, voltage, frequency, and phase angle are continuous outputs, they can be quantized to (discrete) linguistic labels to characterize system safety. The discrete properties are mainly due to the relays, switches and other discrete-dynamic components. In addition, the faults and system maintenances may also lead to different trajectories of system evolution.
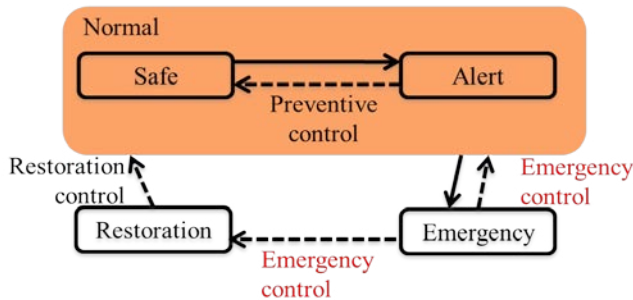

Fig. 2. Schematic of a power system under operation.

Fig. 2 depicts the state transitions of a power system. The system is mostly in state "Safe". Some small disturbance, such as small increment in load, may cause system state transition to "Alert"; large disturbance may transit system state to "Emergency". Emergency control would be required when the system state is in "Emergency".

3.2 Emergency Frequency Control

According to O'Sullivan and O'Malley (1996), the model of power system frequency is given by:

$$\frac{d}{dt}\Delta f(t) \approx \frac{f_0}{2W_{kin0}} \times \left(\Delta P_G(t) - \Delta P_L(t)\right) \quad (7)$$

where $\Delta f(t) = f_0 - f(t)$, $\Delta P_G(t) = P_{G0} - P_G(t)$, $\Delta P_L(t) = P_{L0} - P_L(t)$, W_{kin0} and f_0 are the initial kinetic energy and frequency of the generators, and P_{G0} and P_{L0} are the initial active power of generators and loads.

That is, the system frequency $f(t)$ is a function of $P_G(t)$ and $P_L(t)$. The relationship between the characteristics of active power of load and system frequency is given by (Lin *et al.*, 2008):

$$P_L(t) = P_{LN} \cdot \sum_{i=0}^{\infty} a_i \left(\frac{f(t)}{f_N}\right)^i \quad (8)$$

where P_{LN} denotes the active power load at rated frequency f_N, the loads irrelevant to frequency are constant impedance (such as lights and electric stove), and the induction motors and pumps constitute the power components.

Fig. 3 illustrates primary and secondary frequency regulation of power system at continuous level. In Fig. 3(a), the power frequency characteristics of load (P_L) and generator (P_G) crossover at the initial operating point (f_0, P_0); when there is an increment in load, the power frequency characteristics is shifted up to P_L' (red line); and the new operating point becomes (f_0', P_0'); this is called *primary frequency regulation*. In Fig. 3(b), after primary frequency regulation (blue line), the spinning reserve is released and the power output of generator is increased, the power frequency characteristics of generator is shifted up to P_G' (red line) and the frequency is decreased to f_0''; if the spinning reserve is sufficient to cover the increment in load, the final power frequency characteristics of generator can be shifted up to green line to maintain frequency f_0 (*secondary frequency regulation*).
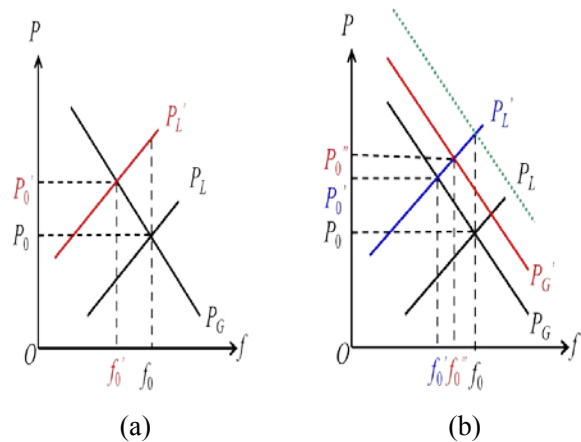

(a)   (b)

Fig. 3. The frequency regulation of power system: (a) primary; (b) secondary.

Both primary and secondary frequency regulations are achieved with automatic generation control (AGC) and generator governor and are applied whenever there is disturbance.

We denote conventional UFLS scheme as Method I. Lin *et al.* (2008) proposed a new UFLS scheme, which is denoted as Method II. Inspired by Method II, we propose the following method (denoted *our method*) for our problem:

Step 1: Divide the load as in Steps 2' and 3' in Method II as follows:

Step 2': Divide the loads as capable of being shed and incapable of being shed.

Step 3': For the loads capable of being shed, divide them as coarsely tuned loads and fine tuned loads:

a) The coarsely tuned loads are larger and cannot be re-closed by UFLS controller;

b) The fine tuned loads are smaller and can be re-closed by the controller.

Step 2: Based on the division, the general input alphabet is {*N, CR, CF, R* }, where *N* stands for doing nothing; *CR* stands for shedding a coarsely tuned load; *CF* stands for shedding a fine-tuned load; and *R* stands for re-closing a fine-tuned load.

Step 3: Perform abstraction of the power system by a DES.

Step 4: Design a supervisor for this DES: for each discrete state, only part of the input alphabet is enabled;

Step 5: Apply FPC to the sub-alphabet and determine the optimal input as follows:

a) If the system can be restored (predicted by the model) with the optimal input, then calculate its settling time t_s (with the prediction), and the time for next action is set to $\Delta t = k \cdot t_s$ with $k \le 1$;

b) If the system cannot be restored, set $\Delta t = t_c$, where t_c is the computational time required by FPC.

Step 6: Loop back to **Step 5**.

4. SIMULATION RESULTS AND ANALYSIS

4.1 Simulation Setup

As an illustrative example, we adopt the IEEE 14-bus test case (Fig. 4), which represents an approximation of the American Electric Power system as of Feb. 1962 and has 14 buses, 5 generators and 11 loads.

The rated power of generators is 120 MW. Set the total consumption of loads as 480 MW + 90 MVA, in which 60% are capable of being shed (red in Fig. 4), namely 288 MW + 54 MVA. Under the same assumption as in Lin *et al.* (2008), 80% of the shedding loads are equally divided to 5 coarsely tuned loads, 46.08 MW + 8.64 MVA each (load L_1 to L_5) and the other 20% are equally divided to 3 fine-tuned loads, 19.2 MW + 3.6 MVA each (load L_6 to L_8). The loads incapable of being shed are L_9 to L_{11}, with $L_9 = 96$ MW + 18 MVA and $L_{10} = L_{11} = 48$ MW + 9 MVA.

Furthermore, to match real industrial loads, the parameters in (8) are set as (Lin *et al.*, 2008) $a_0 = 0.1, a_1 = 0.55, a_3 = 0.35$.

In simulations, the loads weighed by a_0 are simulated by constant impedance and the loads weighed by a_1 and a_3 are simulated by induction motors.
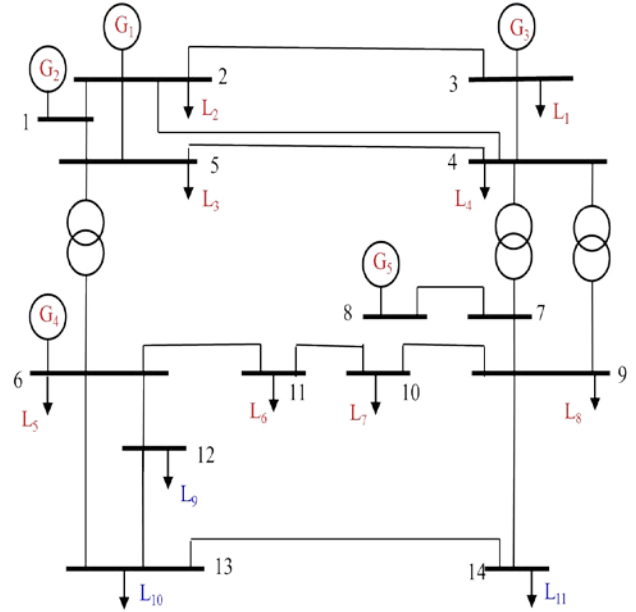

Fig. 4. The IEEE 14-bus test case.

The simulation is carried out for 300 s. At 103 s, generator G_4 is down, leading to a rapid drop in output power. Meanwhile, other generators are slowly releasing their spinning reverse respectively to compensate for the deficiency.

The specifications for emergency frequency control are $t(f \le 47\text{Hz}) \le 0.5$ s , $f(\infty) \ge 49.5$ Hz and $\max_{t \in [0,+\infty)} f(t) \le 51$ Hz .

These control objectives implies that the final value of frequency must fall within the interval [49.5, 51] Hz. Moreover, for economic consideration, the loads need to be shed as little as possible. This additional requirement would also be taken into account in controller design.

4.2 Design of Supervisor

To design the high-level supervisor, the hybrid plant (i.e., power system) must be abstracted to a DES. Using the fuzzy *l*-complete approximation approach proposed in Zhang, Xia and Wang (2018), a fuzzy abstraction of power system can be realized.

Assume that the frequency $f \in \mathbb{R}$ is located in the target interval [49, 51] Hz, then we choose the MFs as (Fig. 5):

$$\mu_{\tilde{A}}(x) = \exp\left[-\frac{(x-50)^2}{0.0144}\right],$$

$$\mu_{\tilde{B}}(x) = \exp\left[-\frac{(x-49.7)^2}{0.0577}\right],$$

$$\mu_{\tilde{C}}(x) = 0.5 - 0.5 * \tanh\left(\frac{x-49.5}{0.04}\right),$$

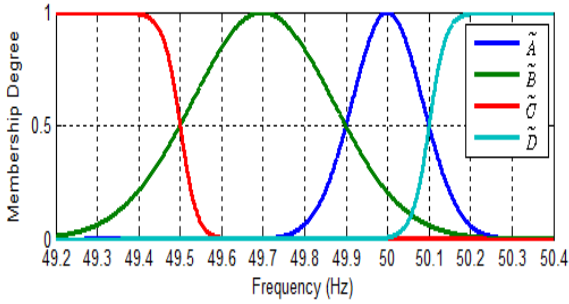$$\mu_{\tilde{D}}(x) = 0.5 + 0.5 * \tanh\left(\frac{x-50.1}{0.04}\right).$$

Fig. 5. The four MFs used by fuzzy abstraction.

The measurement symbol set of system frequency is $[A, B, C, D]$, where $A : f(t) \in (49.9, 50.1)\,\text{Hz}$, $B : f(t) \in (49.5, 49.9]\,\text{Hz}$ and $C : f(t) \in [0, 49.5]\,\text{Hz}$ are *Safe*, *Alert*, and *Emergency* state in Fig. 2, respectively, and $D : f(t) \geq 50.1\,\text{Hz}$ denotes overshooting.

For the state of *Restoration*, the following state set X_f of finite-state machine can be obtained:

$$X_f = \begin{cases} A(A), A(B), A(D), B(A), B(B), B(C), C(B), C(C), D(D), D(A), \\ AA(A), AA(B), AA(D), AB(A), AB(B), AD(A), AD(D), \\ BA(A), BA(B), BA(D), BB(A), BB(B), BB(C), BC(B), BC(C), \\ CB(B), CB(C), CC(B), CC(C), \\ DA(A), DA(B), DA(D), DD(A), DD(D) \end{cases} \quad (9)$$

The state in X_f takes into account both the previous and current output of the system. Moreover, the measurement symbol in round bracket is Guardian State, meaning the potential next output. Then X_f can be divided into four subsets: *Safe*, *Alert*, *Emergency* and *Restor.*. The first three subsets are disjoint, but there are intersections with the last one (*Restoration*), i.e., we have:

$$\text{Safe} = \{A(A), A(B), A(D), AA(A), AA(B), AA(D), DA(A), DA(B), DA(D)\}$$

$$\text{Alert} = \{B(A), B(B), B(C), AB(A), AB(B), BB(B), BB(C)\}$$

$$\text{Emergency} = \{C(B), C(C), BC(B), BC(C), CC(C)\}$$

$$\text{Restor.} = \begin{cases} A(A), A(D), B(A), B(B), C(B), C(C), D(D), \\ AA(A), AA(D), AD(A), AD(D), BA(A), BA(B), BA(D), BB(A), \\ BB(B), CB(B), CB(C), CC(B), CC(C), DD(A), DD(D) \end{cases}$$

Therefore, the supervisor can be designed based on the following four rules:

R[1]: For *Safe* states, nothing is done by UFLS, the control sub-alphabet is $\{N\}$;

R[2]: For *Emergency* states, the sub-alphabet is $\{N, CR, CF\}$;

R[3]: For *Restoration* states, the sub-alphabet is $\{N, CF, R\}$;

R[4]: For *Alert* states, the sub-alphabet is generally $\{N\}$; for the states whose guardian state is C, the sub-alphabet is $\{N, CF\}$.

4.3 Fuzzy Model Predictive Control

As depicted in Fig. 1, the lower-level controller is realized via fuzzy model predictive control. The fuzzy model predictive controller is composed of three components: fuzzy model, prediction, and optimization.

The fuzzy model consists of a collection of fuzzy if-then rules and the associated MF parameters. The Wang-Mendel (WM) method for data-driven fuzzy modelling is used to generate automatically the fuzzy rule base from numeric data. Moreover, particle swarm optimization (PSO) is used to optimize those MF parameters of fuzzy model.

According to (7), $\dfrac{d}{dt}\Delta f(t)$ is dependent on the system inputs $P_G(t)$ and $P_L(t)$; hence fuzzy model has three inputs: $P_G(t)$, $P_L(t)$, and $f(t-1)$. Each I/O domain is partitioned into seven fuzzy subsets. The initial MF parameters are empirically set and then optimized with PSO. The initial setting of PSO algorithm is as follows: 1000 iteration steps, swarm size 20, learning rate $c_1=c_2=1.4972$, inertia weight 0.9. After optimization, the fuzzy partition of each input/output variable (i.e., 3 input and 1 output for the fuzzy model) is shown in Fig. 6 and the fuzzy rule base comprising 18 fuzzy production (if-then) rules is presented in Table 1. The training and testing data is acquired via PSCAD/EMTDC 4.2.0.

4.4 Simulation Results and Discussions

The system output (i.e., frequency) is shown in Fig. 7. At $t_0=103$ s, generator G_4 is down, leading to a rapid drop in output power. This caused an emergency state of the whole system. Meanwhile, other generators are slowly releasing their spinning reverse respectively to make up the deficiency. At $t_1=103.84$ s, the discrete state is evolved from BB(B) to BB(C) and then control needs to be applied. The input sub-alphabet is $\{N, CF\}$, with the fuzzy model we predict that control input CF is the optimal. However, the system cannot be restored by prediction. So after 0.1s (t_c) at $t_2=103.94$ s, a control action still needs to be applied. The discrete state of system is still BB(C), one more fine-tuned load must be shed. Since the power deficiency is much larger than the consumption of two fine-tuned loads, the system cannot be restored immediately.

Table 1. Fuzzy rule-base of the fuzzy model.

$P_G(t)$	$P_L(t)$	$f(t-1)$	$f(t)$
1	1	1	2
1	1	2	3
1	2	2	2
2	1	1	2
3	1	1	2
3	2	3	2
3	2	4	5
3	2	5	5
3	2	6	5
3	2	7	7
5	1	1	2

5	5	1	2
5	5	2	2
5	7	6	5
6	5	2	2
6	7	2	2
6	7	3	2
6	7	6	4
7	7	6	5

(a) $P_G(t)$ (b) $P_L(t)$
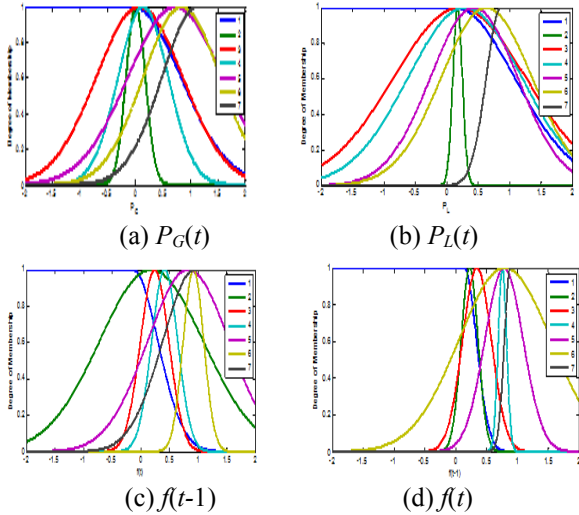

(c) $f(t-1)$ (d) $f(t)$

Fig. 6. The seven fuzzy MFs covering model I/O variables.

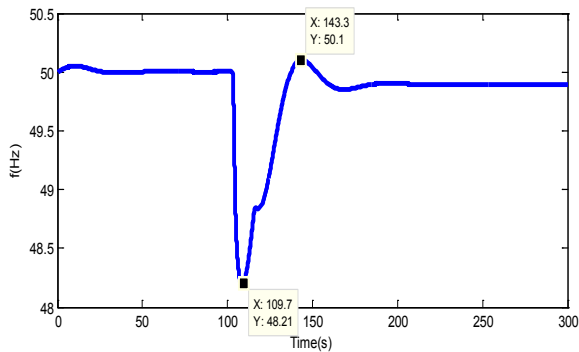
Fig. 7. The simulation result of UFLS by our method.

After a time delay of 0.1s, at t_3=104.04s the discrete state of system becomes CC(C) and the input sub-alphabet is then {N, CR, CF}; CR is selected because it would restore the system. Hence we adopt CR and calculate the settling time t_s and chose $\Delta t = \frac{1}{4} \cdot t_s$ as the holding time of control input CR. Fig. 8 shows the model prediction with control input CR. $\Delta t = \frac{1}{4} * (149.24 - 104.04) = 11.3$ s. Then at $t_4 = 104.04+11.3 = 115.34$ s, the system state belongs to *Restor.* and the input sub-alphabet is {N, CF, R}. With performance optimization, the control input R performs the best even with selection of different weights in performance index (see Table 2).

We present the simulation results of Method I and Method II:

Method I: Set the frequency thresholds f_i = 49 Hz, f_j = 49.5 Hz and frequency step size f_{step} = 0.3 Hz, the simulation result is shown in Fig. 9(a).

Method II: Set the pick-up frequency f_1 = 49.2 Hz and frequency change rate thresholds $F_f = 1.8$ Hz/s, $F_{rs} = -0.15$ Hz/s, $F_{rf} = -1$ Hz/s ; K_q = 70%, $K_p = 0.5, K_I = 0.5, K_D = 2$ as in Lin *et al.* (2008), the simulation result is shown in Fig. 9(b).
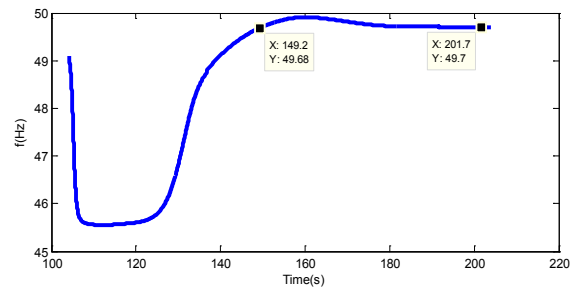

Fig. 8. Model prediction at t_3=104.04 s with control CR.

Table 2. Performance index under different weights.

(w_1, w_2)	CF	N	R
(0.1,0.9)	0.8420	0.8610	**0.8793**
(0.2,0.8)	0.8380	0.8573	**0.8753**
(0.3,0.7)	0.8341	0.8535	**0.8712**
(0.4,0.6)	0.8301	0.8498	**0.8671**
(0.5,0.5)	0.8261	0.8461	**0.8630**
(0.6,0.4)	0.8222	0.8424	**0.8590**
(0.7,0.3)	0.8182	0.8387	**0.8549**
(0.8,0.2)	0.8143	0.8350	**0.8508**
(0.9,0.1)	0.8103	0.8313	**0.8467**

At t_0=103 s, generator G_4 is down, the instantaneous power deficiency is 83 MW, so when $f(t_1)$=49.1791 Hz < 49.2 Hz at t_1=104.16 s, an amount of load mostly approaching to 83*70%=58.1 MW should be shed, so one coarsely tuned load (48 MW) and one fine-tuned load (10 MW) are simultaneously shed after a delay of 0.2s. The next execution time is calculated by PID algorithm as Δt=0. 4183 s. So at t_2=104.78 s, $d\Delta f/dt$ =1.1351 Hz/s , $-0.15 = f_{rs} < d\Delta f/dt = 1.1351 < f_F = 1.8$, another fine-tuned load should be shed. The next execution time is t_3=105.28 s, $-0.15 = f_{rs} < d\Delta f/dt = 0.7862 < f_F = 1.8$, one more fine-tuned load should be shed.

Then the five control performance indices (i.e., settling time t_s, overshoot, duration of emergency state, steady-state frequency $f(\infty)$, and peak frequency f_{max}) of Method II and our method is compared in Table 3.
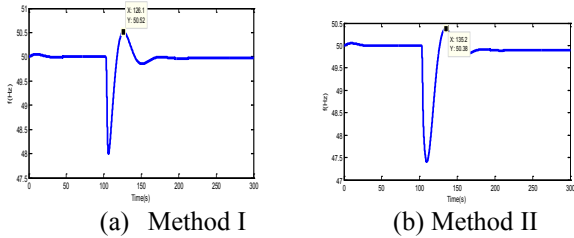
(a) Method I   (b) Method II

Fig. 9. Simulation results of two existing UFLS methods.

Table 3. Comparison of control performance between Method II (Lin *et al*., 2008) and our method.

	t_s [s]	Overshoot [%]	duration of emergency state [s]	$f(\infty)$ [Hz]	f_{max} [Hz]
Method II	61.7	1.09	10.72	49.97	50.52
Our method	75.24	0.42	25.34	49.89	50.10

Interestingly, if we re-close a fine-tuned load at time t_3, (similar to the last step in our method) the simulation result is displayed in Fig. 8. We can observe that the system frequency can also be restored, with $t_s = 69.66$ s, overshoot 0.97%, duration of emergency state 19.28 s, $f(\infty)$=49.89 Hz, and f_{max}=50.38 Hz. However, more load can be kept during restoration, implying better economic gains.

By comparing the control performance indices, we can see that Method II can restore the system faster than our method but with larger overshooting, which may negatively impact the stable operation of the whole power system. Moreover, if we take into consideration both frequency and output power, we can find that the proposed method is superior to other two methods from Table 4.

Table 4. Performance comparison of three UFLS methods.

(w_1,w_2)	Method I	Method II	Our Method
(0.1,0.9)	0.8443	0.8747	0.8793
(0.2,0.8)	0.8434	0.8646	0.8753
(0.3,0.7)	0.8425	0.8546	0.8712
(0.4,0.6)	0.8416	0.8445	0.8671
(0.5,0.5)	0.8406	0.8344	0.8630
(0.6,0.4)	0.8397	0.8244	0.8590
(0.7,0.3)	0.8388	0.8143	0.8549
(0.8,0.2)	0.8379	0.8043	0.8508
(0.9,0.1)	0.8370	0.7942	0.8467

5. CONCLUSIONS

In this paper, we proposed a hierarchical control approach for hybrid system with discrete inputs. We firstly abstract the system to a DES. Then we design a supervisor in the higher level to provide legal control input alphabet for each discrete state and a fuzzy model predictive controller in the lower level to select the optimal control symbol for the original system. Simulation results showed that the proposed hierarchical control scheme leads to superior frequency recovery characteristic of the UFLS.

REFERENCES

Azuma, S.I. and Sugie, T. (2008). Synthesis of optimal dynamic quantizers for discrete-valued input control. *IEEE Trans. on Automatic Control* 53(9), pp. 2064-2075.

Bemporad, A. and Morari, M. (1999). Control of systems integrating logic, dynamics, and constraints. *Automatica*, 35(3), pp. 407–427.

Feng, L. and Wonham, W.M. (2008). Supervisory control architecture for discrete-event systems. *IEEE Trans. on Automatic Control*, 53(6), pp. 1449-1461.

Howlett, P. (2000). The optimal control of a train. *Annals Operations Research*, 98(1–4), pp. 65–87.

Ikeda, T., Nagahara, M. and Ono, S. (2017). Discrete-valued control of linear time-invariant systems by sum-of-absolute-values optimization. *IEEE Trans. on Automatic Control* 62(6), pp. 2750-2763.

Lin, X. *et al*. (2008). The frequency closed-loop control strategy of islanded power systems. *IEEE Trans. on Power Systems,* 23(2), pp. 796-803.

Minami, Y. (2016). Design of model following control systems with discrete-valued signal constraints. *Int. J. of Control Automation & Systems* 14(1), pp. 331-339.

O'Sullivan, J.W. and O'Malley, M.J. (1996). Identification and validation of dynamic global load model parameters for use in power system frequency simulations. *IEEE Trans. on Power Systems*, 11(2), pp. 851–857.

Raisch, J. and O'Young, S.D. (1998). Discrete approximation and supervisory control of continuous systems. *IEEE Trans. on Automatic Control,* 43(4), pp. 569-573.

Ramadge, P.J. and Wonham, W.M. (1987). Supervisory control of a class of discrete event systems. *SIAM J. Control and Optimization*, 25, pp. 206-230.

Ramadge, P.J. and Wonham, W.M. (1989). The control of discrete event systems. *Proc. of IEEE*, 77, pp. 81-98.

Thomas, J. (2012). Analytical non-linear model predictive control for hybrid systems with discrete inputs only. *IET Control Theory & Applications*, 6(8), pp. 1080-1088.

van Der Schaft, A.J. and Schumacher, J.M. (2000). *Introduction to Hybrid Dynamical Systems*. Springer.

Wang, L.-X. (2003). The WM method completed: A flexible fuzzy system approach to data mining. *IEEE Trans. on Fuzzy Systems*, 11(6), pp. 768–782.

Wang, L.-X. and Mendel, J. (1992a). Fuzzy basis functions, universal approximation, and orthogonal least-squares learning. *IEEE Trans. on Neural Networks*, 3(5), pp. 807–814.

Wang, L.-X. and Mendel, J. (1992b). Generating fuzzy rules by learning from examples. *IEEE Trans. on Systems, Man, and Cybernetics*, 22(6), pp. 1414–1427.

Wonham, W.M. and Ramadge, P.J. (1988). Modular supervisory control of discrete-event systems. *Mathematics of Control Signals & Systems*, 1, pp. 13-30.

Woon, S.F., Rehbock, V. and Loxton, R. (2012). Towards global solutions of optimal discrete-valued control problems. *Optimal Control Appl. Methods*, 33(5), pp. 576–594.

Zhang, J., Xia, J. and Wang, R. (2018). Modelling and supervisory control of hybrid dynamical systems via fuzzy l-complete approximation approach. *Nonlinear Analysis: Hybrid Systems*, 27, 390–415.